Noname manuscript No.
(will be inserted by the editor)

Predictability of intraspecific size variation in extant planktonic foraminifera

Marina C. Rillo · C. Giles Miller · Michal Kučera · Thomas H. G. Ezard

Received: date / Accepted: date

Abstract Planktonic foraminifera (PF) size varies greatly both among and within species. This variation affects our understanding of PF ecology and evolution as well as reconstructions of the ocean-climate system. It is currently accepted that PF species are largest under optimum environmental conditions, where abundance is maximised. This idea is based on observations from marine sediment assemblages; however, these observations either had limited intraspecific resolution or focused on a restricted part of each species' biogeographical range. Here we compile a new global PF shell size dataset to investigate the relationship between intraspecific size variation and abundance and sea surface temperature (SST). Our dataset contains 3817 individual size measurements on nine PF species in 53 surface sediments around the world. For each species, we fitted a generalised linear model of population shell size as function of local abundance (as an indicator of optimum environmental conditions) and SST. We support previous results that species maximum size and maximum abundance rank along SST; however, this relationship is not supported within species. Only two species out of nine revealed a significant positive relationship between size and abundance, suggesting shell size is not maximised at the species environmental optimum. SST significantly explained variation in shell size for four species out of nine. By incorporating intraspecific variation and sampling broader geographical ranges compared to previous studies, we conclude that the relationships between PF shell size and abundance or SST are either absent or weaker than previously reported.

Keywords ecological optimum · relative abundance · macroecology · biogeography of traits · morphometrics · natural history collection (NHC)

Marina C. Rillo
National Oceanography Centre Southampton, University of Southampton, SO14 3ZH, UK
Department of Earth Sciences, Natural History Museum, Cromwell Road, London SW7 5BD, UK
E-mail: marina.rillo@evobio.eu

C. Giles Miller
Department of Earth Sciences, Natural History Museum, Cromwell Road, London SW7 5BD, UK

Michal Kučera
MARUM, University of Bremen, Leobener Strasse, 28359, Bremen, Germany

Thomas H. G. Ezard
National Oceanography Centre Southampton, University of Southampton, SO14 3ZH, UK

1 Introduction

Organism size is a functional trait that influences biological processes across multiple levels of organisation: from individual physiology (Brown et al., 2004) and interactions (Emmerson and Raffaelli, 2004; Berlow et al., 2009) to populations (Damuth, 1981; Peters and Wassenberg, 1983; Jennings and Mackinson, 2003; Savage et al., 2004; Reuman et al., 2008), communities (Woodward et al., 2005; Petchey et al., 2008; Boyce et al., 2015; Gianuca et al., 2016) and ecosystems (Barton et al., 2013; Boyce et al., 2015). More specifically, size variation within species can affect species coexistence (Hart et al., 2016) and species' responses to environmental change in marine communities (Sommer et al., 2017; Mousing et al., 2017). The ecological importance of trait variation within species is prominent (Bolnick et al., 2011; Violle et al., 2012; Des Roches et al., 2018), suggesting that our understanding of marine ecosystems might be incomplete when examined only at the level of species.

Planktonic foraminifera (PF) are single-celled eukaryotes that produce calcium carbonate tests (or shells, Kucera 2007) and are ubiquitous in the marine pelagic environment. PF species vary remarkably in size, from diameters in the order of 1 μm (Morard et al., 2018) up to 10^4 μm (the species *Hastigerina pelagica* can reach diameters of 2.5 cm when alive; Anderson and Be 1976). Among adults within a species, PF shell size variation can range over one order of magnitude (from 150 μm to 1500 μm, *Globorotalia menardii*; this study). PF shell size increases during its lifetime until reproduction (gametogenesis), after which the dead, empty shell sinks to the ocean floor (Be and Anderson, 1976; Hemleben et al., 1989). PF shells compose much of the marine sediments yielding not only a uniquely complete fossil record (Ezard et al., 2011) but also the most common proxy of past oceanic environments (Kucera, 2007). Therefore, quantifying and discerning what controls PF intraspecific size variation could improve not only our understanding of PF ecology and macroevolution, but also our palaeoclimate reconstructions.

It is currently accepted that PF species reach largest average sizes under environmental conditions to which they are optimally adapted, defined as the species' ecological optima. This idea is based on observations from marine sediments, which showed that areas of population maximum shell size often coincide with the areas of maximum relative abundance of each species (Kennett 1976; Hecht 1976; Malmgren and Kennett 1976, 1977; Kahn 1981; Schmidt et al. 2004; Moller et al. 2013; but see Be et al. 1973). However, these studies have either focused on a single oceanic basin and thus a limited part of each species' range, or were based on small sample of taxonomically classified individuals.

In theory, the species' ecological optimum represents the environmental conditions where the average fitness of the population is maximised (Kirkpatrick and Barton, 1997). Optimal fitness, however, is hard to quantify, as there are trade-offs among fitness components (*e.g.*, feeding, survival, growth, reproduction; Orr 2009) and thus all cannot be maximised simultaneously (Litchman et al., 2013). In practice, the species' ecological optimum is usually defined as the local environmental conditions where its population reaches maximum abundance (Kirkpatrick and Barton, 1997; Sagarin and Gaines, 2002; Liancourt et al., 2005; Wang et al., 2008; Rehfeldt et al., 2018). The underlying assumption is that higher average fitness of the population means that, on average, individuals have more energy to invest in feeding, survival, growth and reproduction and, therefore, contribute relatively more to future generations at the local optimum than elsewhere, yielding higher local abundances (Orr, 2009).

PF local population abundance is usually estimated by counting assemblages from seafloor surface sediments. This methodology yields relative abundance data with respect to the

counted assemblage (*i.e.*, other co-occurring species) rather than absolute abundance, as the latter cannot be retrieved from sediment samples without precise knowledge of the local sedimentation rate. Absolute abundance could be recovered by sampling the surface waters. The disadvantages of using water sampling methods to estimate species local absolute abundance is that the water samples either represent an instant snapshot of the planktonic seasonal dynamics (plankton nets) or could be subject to large interannual variability (sediment traps) (Weinkauf et al., 2016). Nevertheless, analyses of absolute abundance data from direct water sampling did not find support for a positive relationship between population shell size and abundance (Beer et al., 2010; Aldridge et al., 2012; Weinkauf et al., 2016), challenging the idea that PF intraspecific size variation can be predicted by population abundances.

Alternatively, PF size variation could be predicted by physical and chemical properties of the seawater. Abiotic factors such as temperature, salinity, nutrient availability, carbonate saturation and oxygen availability are known experimentally to influence PF final shell size (Be et al., 1981; Caron et al., 1981, 1987b,a; Hemleben et al., 1987; Bijma et al., 1990b, 1992). In the open ocean, most of these environmental variables are highly correlated and difficult to disentangle (Schmidt et al., 2006; Aldridge et al., 2012; Fenton et al., 2016). Sea surface temperature (SST) appears to be the most important abiotic parameter affecting PF assemblage size structure (Schmidt et al., 2004) and, more generally, PF spatial diversity patterns (Rutherford et al., 1999; Morey et al., 2005; Tittensor et al., 2010; Fenton et al., 2016). Thus, if PF shell size responds to optimum SST in a predictable way, we can expect shell size to *(i)* decrease with increasing SST for polar species, *(ii)* reach largest values at intermediate SST for transitional species, or *(iii)* increase with increasing temperature for tropical species (Schmidt et al., 2006). Moreover, the SST at which PF species reach largest size and highest relative abundance have been shown to coincide (Schmidt et al., 2004), supporting the idea that PF reach largest shell size at the species ecological optimum (Hecht, 1976).

Here we explore for the first time in a global biogeographical scale how population-level PF size relates to local relative abundance and SST. We built a new intraspecific shell size dataset for nine extant PF species, extracted from a recently digitised museum collection (Rillo et al., 2016). Our data comes from seafloor sediments, which averages short-term fluctuations in abundance that potentially blur macroecological patterns (Fenton et al., 2016). We spatially associate our morphometric data with population-level relative abundance data and local SST data to test: *(i)* whether PF populations are largest where they are most abundant, *(ii)* what is the relationship between SST and PF within-species size variation and *(iii)* if the SST values at which a species reaches maximum size and maximum relative abundance coincide (as found by Schmidt et al. 2004).

2 Material and Methods

Our PF size dataset was extracted from the recently digitised Henry Buckley Collection of Planktonic Foraminifera (Rillo et al., 2016), held at The Natural History Museum in London (NHMUK). We measured shell area of 3817 individuals from the nine extant PF species most commonly represented in the collection across 53 sites worldwide (Fig. 1). We obtained corresponding open-access data on the relative abundance of each species (Siccha and Kucera, 2017) and mean annual values of SST (Locarnini et al., 2013) for each sampled site.

2.1 Study sites and samples

Henry Buckley sampled 122 marine sediments from the NHMUK Ocean-Bottom Deposits Collection (OBD) to amass the NHMUK Henry Buckley Collection of Planktonic Foraminifera (Rillo et al., 2016). From these sea-floor sediment samples, we selected those that contained only modern species (Table S2), were collected within the upper 15 cm of sediment, and included at least one of the nine focal species (see below). This resulted in 53 study sites covering the major physical and chemical gradients of the world's oceans (Fig. 1a). Our sample sites are predominantly in the Pacific and Indian oceans, as opposed to the study of Schmidt et al. (2004), which had more samples in the Atlantic ocean. The 53 sediment samples used in our study were collected by historical marine expeditions between the years of 1873 and 1965 (Table S1), and have been shown to be representative of the Holocene (Rillo et al., 2018).

We determined the water depth for each site by matching the collection's reported latitudes and longitudes to the ETOPO1 database hosted at the National Oceanic and Atmospheric Administration website (Amante and Eakins, 2009) using a 2 arc-minute grid resolution (R package *marmap* version 0.9.5, Pante and Simon-Bouhet 2013). Water depth ranged from 746 to 5153 meters below sea level (median 3296 m).

2.2 Shell size data

We measured shell area of the nine most abundant PF species in the NHMUK Henry Buckley Collection of Planktonic Foraminifera, all having at least 244 specimens in the collection, resulting in 3817 individual measurements (Table 1, S1). Brombacher et al. (2018) recently showed that PF shell area provides a consistent proxy for shell volume, and thus a more realistic estimation of organism size. The species *Globigerinoides ruber* (white), *G. ruber* (pink) and *G. elongatus* (Aurahs et al., 2011) were analysed together as *G. ruber*.

The specimens of the collection were imaged using a Zeiss Axio Zoom V16 microscope and ZEN software at a resolution of 2.58 μm x 2.58 μm per pixel. Individual size was estimated based on the two-dimensional image of the specimen using the software Image-Pro Premier (version 9.1), which automatically recognises each specimen and measures its shell area. This automated individual recognition is based on the contrast between the white shell and the black background of the slide. However, there was differential fading through the years of slide backgrounds of the Buckley Collection, which impeded the use of the same automated contrast threshold. Thus, the contrast threshold was inspected for each image and, when necessary, altered in order to precisely measure the shell contour of the specimen.

Henry Buckley mounted most specimens on the slides in a standard orientation (Fig. 1b, Table 1); individuals that had a different orientation or dubious taxonomic identification were excluded from the analysis. The Buckley Collection could have a collector effort bias towards larger (or smaller) specimens. To assess this potential bias, we re-sampled ten original bulk sediments from the OBD Collection that Buckley had used to amass his collection (Fig. 1a, Section S3). We mounted species-specific slides from the re-sampled samples and extracted shell size data in the same way as for the slides of the Buckley Collection. The comparison of the shell size distributions between the re-sampled and Buckley's samples included 2873 individuals (1824 from the re-sampled samples and 1049 from the Buckley Collection) from 20 species collected from the ten sites, 65 populations in total (Section S3). We log-transformed the shell data and calculated the mean, median, 75th percentile, 95th percentile and maximum value of each population shell size distribution. We then regressed

each of these five population metrics of the Buckley Collection against the re-sampled data, and calculated the residuals based on the identity function (1:1 relationship). The residuals of the regressions were predominantly positive (Fig. S2), indicating that the Buckley Collection has a consistent collector bias towards large specimens.

The mean squared error was lowest for the 95th percentile (Fig. S2), meaning that this metric is the most representative population metric of the Buckley Collection. The robustness of the size distribution's 95th percentile has also been documented by Schmidt et al. (2004), as it is less sensitive to single outliers than the distribution's maximum value, and to representative sampling at the lower end of the size range than the distribution's mean and median values. Accordingly, in our analyses, we used the 95th percentiles of the population shell size distributions as the dependent variable to investigate what controls PF intraspecific shell size variation. As Henry Buckley personally carried out all the sample processing, isolation of foraminiferal specimens and their identification, the collector biases in his collection are likely to be systematic for within-species comparisons.

2.3 Relative abundance data

To test the relationship between population shell size and abundance, we extracted assemblage composition data from the ForCenS open database (Siccha and Kucera, 2017). This database is a synthesis of PF assemblage counts from surface sediment samples, with 4205 records from unique sites worldwide, each with corresponding information on species relative abundance. We assume that relative abundances of species match their absolute abundances. This assumption is supported by studies of Beer et al. (2010) and Weinkauf et al. (2016), who found consistency between analyses using both relative and absolute population abundances. Moreover, long-term sediment traps, which would average out inter-annual variability and thus be ideal for absolute abundance estimation, are not available on the geographic resolution of our morphometric dataset especially in the Pacific Ocean (see Jonkers and Kucera 2015).

The spatial arrangement of dead PF on the sea floor is affected during settling by subsurface currents (Berger and Piper, 1972). Recent models estimate that dead foraminiferal shells can travel a maximum distance of 300 km in regions with largest horizontal velocities along the equator, in the western boundary currents and in the Southern Ocean (Van Sebille et al., 2015). To account for this post-mortem spatial variation of foraminiferal abundance on the sea floor, we retrieved ForCenS assemblage data within a 300 km radius distance of each morphometric sample coordinate. We then calculated the median relative abundance for each species based on all ForCenS samples that fell within the 300 km distance of each morphometric sample. The distances between the datasets were calculated considering the World Geodetic System of 1984 (WGS 84) (R package *geosphere* version 1.5-7, Hijmans 2015).

To test for the effect of retrieving relative abundance data of samples 300 km apart, we ran the same analysis using solely the nearest neighbour of the ForCenS database relative to each morphometric sample. The median distance between the morphometric samples and their nearest ForCenS neighbours was 106 km. The analyses using the single nearest ForCenS sample produced consistent results when compared to the analyses using all samples within a 300 km distance (Section S5). We present results using the more conservative 300 km median relative abundance.

2.4 Sea surface temperature data

We compiled mean annual values of sea surface temperature from the World Ocean Atlas 2013 (WOA13, 0 meters depth, Locarnini et al. 2013) for each morphometric sample by matching its unique latitude and longitude coordinates to the nearest WOA13 1° grid point (1° is approximately 111 km at the equator). Again, the distances between the datasets were calculated using the WGS 84 system (Hijmans, 2015). We used SST data from the earliest decade available in the WOA13 database, resulting in SST data averaged for the years between 1955 and 1964. We chose this time period because the last historical expedition that we used for our morphometric dataset sailed in 1965 (Table S1).

2.5 Statistical analysis

Effects of relative abundance and sea surface temperature on PF population shell size distributions were assessed using generalised linear models (GLM) with the Gamma error distribution to correct the shell area distributions. The logarithmic link function was used for consistency with our later analyses. For each species, the dependent response variable was the 95th percentile of the population size distribution whereas the independent explanatory variables were the local relative abundances (median within 300 km distance) and mean annual SST. We compared the GLM models through a hierarchical model selection framework. We started all analyses with a null model that included the population shell size as the dependent variable and the regression parameter constant (sample mean). We then added the predictor variable(s) to this model incrementally to see whether the model was improved. Adjusted R-squared (R^2_{adj}) were calculated for each GLM model (R package *rsq* version 1.0.1, Zhang 2017). Model fit was assessed using Akaike information criterion corrected for small sample size (AICc, R package *MuMIn* version 1.40.0, Barton 2017).

We also investigated the general relationship between PF shell size and relative abundance and SST using linear mixed-effects regression (LMER) (R package *lme4* version 1.1.15, Bates et al. 2015). The log-transformed 95th percentile of the population shell size distributions was modelled as the response variable, and the independent fixed variables (effects) were the local relative abundances (median within 300 km distance) and the mean annual SST. We log-transformed the shell size variable and used a normal error distribution because a generalised linear mixed-model (GLMM) would not converge for our data. Species were modelled as random effects, allowing for random intercepts and slopes (*i.e.*, the intercept and slope of the relationship between shell size and the fixed effects may vary among species). We used the Likelihood Ratio Test (LRT) to compare the likelihood of each fixed effect (including interactions between effects). For each possible added fixed effect, we calculated the LRT between the models with and without the effect. Significance of each fixed effect was given through the LRT. Marginal R^2 (R^2_m), which refers to the fixed effects, was calculated for each LMER.

3 Results

In general, intraspecific size variation is high among populations (Fig. 2) and within populations (Fig. S3). Among the nine PF species studied, only *T. sacculifer* and *G. truncatulinoides* show a statistically significant positive relationship between shell size and relative

abundance. Relative abundance never explains more than 7% of population shell size variation (R^2_{adj} in Fig. 2a). Regarding mean annual SST, *T. sacculifer*, *G. siphonifera* and *P. obliquiloculata* increase in size significantly with linear increase of SST (Fig. 2b) while *G. truncatulinoides* intraspecific shell size variation is significantly explained by a quadratic function of SST. Shell size in the other five species did not covary significantly with SST.

No GLM with relative abundance as the sole explanatory variable was the best-supported model (Table 2). Although relative abundance alone significantly explains shell size variation within *T. sacculifer* and *G. truncatulinoides* (Fig. 2a), the best supported model for *T. sacculifer* and *G. truncatulinoides* includes only SST, and adding abundance data has no impact or decreases the amount of intraspecific size variation explained by the SST model (R^2_{adj} in Table 2). *G. menardii*'s best supported model was the full GLM of both variables (abundance and quadratic SST) plus their interaction term (Table 2), with ΔAICc > 2 and high model weight (Table 2). *G. ruber* and *G. conglobatus* show equal or similar weights between the null and the relative abundance models; however, relative abundance does not significantly explain shell size variation in these two species when tested alone (Fig. 2a). In *N. dutertrei* and *G. inflata*, intraspecific variation was best explained by the null (intercept-only) model with R^2_{adj} below 3% (Table 2). Visual inspection of the residual plots did not reveal any obvious deviations from homoscedasticity, except for *G. inflata* (Fig. S4i).

The LMER shows that relative abundance and linear SST are both significant fixed effects explaining PF population shell size variation (Table 3). The deviance of the data to the models with only SST or abundance is almost equal (both around 112), but by adding both explanatory variables the deviance decreases (to 104), showing that there is an additive effect of SST and abundance (Table 3). The interaction between SST and abundance is not significant.

We used the observations in the 53 samples to determine the SST at which each species reaches its largest size (95th percentile of the population) and the SST at which each species is most abundant. We expected to see a positive species-level relationship as found by Schmidt et al. (2004). Although our data shows a positive trend (Fig. 3), the linear relationship is not significant (linear regression, $R^2_{adj} = 0.11$, $P = 0.198$) with lower R^2_{adj} value compared to the value of 0.98 found in Schmidt (2002). We also find a markedly higher mean squared error (MSE = 19.07) with respect to the identity function when compared to the MSE of 1.34 of the Schmidt (2002) data (Fig. 3).

Lastly, we also used all our 53 observations to get the values of median population shell size and median relative abundance for each species. When these two variables are plotted against each other, they show a negative relationship (Fig. 4), indicating that the species that reach average larger sizes are generally less abundant (relatively) than smaller species.

4 Discussion

Our new global dataset of planktonic foraminifera shell size allowed us to explore the predictability of PF intraspecific size variation. Contrary to the common perception that PF species are largest where they are most common (Hecht, 1976; Schmidt et al., 2004), the relative abundance of a species was in general a poor predictor of its size variation: only two (*T. sacculifer* and *G. truncatulinoides*) of the nine species analysed (Fig. 2a) exhibited a statistically significant relationship between size and abundance. Moreover, adjusted R squared values were low for all species (maximum reached: 0.07) and the relative abundance model was not the best supported model for most of the species analysed (Table 2).

Sea surface temperature explained more PF shell size variation than relative abundance (Fig. 2b, Table 2). *T. sacculifer*, *G. siphonifera* and *P. obliquiloculata*, which are tropical-subtropical species (Kucera, 2007), showed a positive linear relationship between SST and shell size. Moreover, the transitional *G. truncatulinoides* showed a quadratic relationship between shell size and SST (Table 2). These results support the idea that PF species are largest at their environmental temperature optimum (Hecht, 1976; Schmidt et al., 2004, 2006). However, the other analysed species (namely *G. ruber*, *G. conglobatus*, *G. menardii*, *N. dutertrei* and *G. inflata*) showed neither a linear nor quadratic relationship between shell size and SST (Fig. 2b, Table 2), contrary to the expectation of the ecological optimum hypothesis. The definition of optimal temperature range for a species is based on their relative abundances in the marine sediments, with higher relative abundances indicating more optimal temperatures (Kucera, 2007). Thus, although SST could explain more intraspecific shell size variation than local abundance, a positive monotonic relationship between shell size and relative abundance of a species would still be expected under the ecological optimum hypothesis, regardless of the species' biogeography.

When increasing model power by analysing all the species together under a LMER framework, relative abundance is a significant explanatory variable of PF intraspecific shell size variation (Table 3). A linear positive relationship between shell size and SST is also significant (Table 3), even though the LMER includes species with multiple biogeographical preferences (Kucera, 2007). This observation, alongside the contrast between the results from LMER models and the overall GLM models, suggest that the significance of the LMER models are being leveraged by few species' size variation patterns because of the small number of random effects (*i.e.*, species).

4.1 Potential biases in the museum collection

It might be that we did not find a strong relationship between size and abundance within species because of the collector biases found in the NHMUK Henry Buckley Collection of Planktonic Foraminifera (Fig. S2). Another concern regarding our analyses is that we used relative abundance data from the ForCenS database (Siccha and Kucera, 2017) instead of the abundance data estimated from the sediment samples used in the shell size data. As a result, sometimes the ForCenS database yielded 0% of relative abundance of a species in the same region that we had size data for the given species (Fig. 2a). Considering these two issues, we assessed the robustness of our results by testing the same hypothesis on a more uniform, but smaller, dataset. We re-sampled ten original sediment samples used by Buckley to amass his collection (same samples used in the shell size bias analysis, Fig. 1a). We identified, counted and measured the size of all PF individuals in each of the ten samples (Section S3), minimising therefore any potential collector bias. Relative abundances of species were calculated from each re-sampled assemblage itself, meaning that the same specimens were used to extract abundance and size data. We then tested if population shell size could be predicted by relative abundance in this re-sampled dataset using a linear-mixed effect model with species as random effects. The re-sampled dataset included 20 species, summing 65 populations from the ten sites. The results showed no significant relationship between size variation and relative abundance (Chi-square test, $\chi^2 = 2.18$, $P = 0.14$, Table S4), supporting our previous findings using the global Buckley Collection data and our statistical models.

Another source of bias in the Buckley Collection is that the samples come from different expeditions using different sediment sampling strategies (Table S1). This source of bias is inherent to this historical collection, as it includes samples from pioneering marine expedi-

tions such as the *HMS* Challenger (1872−76) which lay on the foundation of oceanography and ocean-floor sampling. In a previous study (Rillo et al., 2018), we showed that the PF assemblages estimated from these historical samples are representative of Holocene assemblages and can, therefore, be used in macroecological studies.

Ten of the 53 samples in our dataset come from sediments prone to dissolution (*i.e.*, waters deeper than 4000 meters for newly sedimented foraminifera, Berger and Piper 1972). Dissolution may affect species size distributions, as smaller individuals are more prone to dissolution (Kennett, 1976; Be and Hutson, 1977). We tested if water depth could explain population shell size variation using a linear-mixed effects model with species as random effects and found that water depth is not significantly related to PF size variation in our dataset (Chi-square test, χ^2 = 1.83, P = 0.18, Table S5).

4.2 Cryptic species

It is possible that some species in our morphological dataset are in fact complexes of lineages, which are genetically independent but morphologically similar (De Vargas et al., 1997; Darling and Wade, 2008). These ”cryptic species” may have different geographical distributions (De Vargas et al., 1999), occupy different niches (Darling and Wade, 2008) and/or display different relationships between size and abundance and SST. It has been shown that many of these cryptic species are endemic to particular ocean basins (Darling and Wade 2008; De Vargas et al. 1999; and references below), so increasing the geographical range of the sampling would also increase the coverage of the cryptic diversity within our morphologically-defined species. Among the nine tested species, *T. sacculifer* and *G. conglobatus* are genetically homogeneous (Aurahs et al., 2011; Seears et al., 2012; Andre et al., 2013). The size-abundance-SST relationship in these species is not markedly different from the species with cryptic diversity, namely *G. inflata* (Morard et al., 2011), *G. ruber* (Aurahs et al., 2011), *G. siphonifera* (Seears et al., 2012; Weiner et al., 2014), *G. truncatulinoides* (Quillevere et al., 2013) and *P. obliquiloculata* (Ujiie et al., 2012). Therefore, the lack of relationship between size and relative abundance and SST does not seem to be explained by the presence of cryptic species. Schmidt et al. (2004) suggested that peaks in maximum population shell size at distinct SST could relate to the species' cryptic phylogeography.However, the high variability in shell size among and within populations found in our study obscured any potential multimodal shell size distributions across the SST range (Fig. 2, Fig. S3).

4.3 Species *vs.* population-level patterns

The idea that species are largest at their ecological optima is recently based on the comparison of temperatures where a species reaches maximum sizes and the temperatures where it reaches maximum relative abundance (see Schmidt et al. 2004). Our species-level comparison showed a positive but not significant relationship between SST of maximum size and abundance (Fig. 3). Although the non-significance of our regression is probably partially due to the absence of sub polar and polar species in our dataset (*e.g. G. bulloides*, *N. incompta* and *N. pachyderma*), our mean squared error with respect to the identify line was strikingly larger than the one of the Schmidt (2002) (Fig. 3). Moreover, species close to the identity line in Fig. 3 do not show a significant relationship of size and abundance at the population-level (Fig. 2a). This result shows that contrasting patterns may be found when analysing

different organizational levels, and emphasizes the importance of intraspecific variation. Indeed, recent evidence has been accumulating showing that variation within species is crucial for our understanding of macroecological and evolutionary patterns (Bolnick et al., 2011; Violle et al., 2012; Hart et al., 2016) and sometimes even surpasses the community-level effects related to variation among species (Mousing et al., 2017; Des Roches et al., 2018).

Another way of looking at species-level patterns is to plot the median population shell size against median relative abundance. PF species showed a negative relationship between size and relative abundance (Fig. 4). Abundant species such as *G. ruber* and *G. inflata* reach smaller average sizes when compared to less abundant species such as *G. conglobatus* and *G. truncatulinoides*. The trade-off between size and abundance is a known macroecological pattern (Damuth, 1981; Woodward et al., 2005; White et al., 2007; Yvon-Durocher et al., 2011; Villarino et al., 2018). Larger organisms have higher nutrient requirements and thus, for a given amount of resources, have slower growth rates and obtain lower population densities than smaller organisms (Fenchel, 1974; Muller and Geller, 1993; Savage et al., 2004; Huete-Ortega et al., 2012). It remains to be tested whether smaller PF species have indeed faster population growth rates.

At population-level, the mechanism that would lead to simultaneous increase of cell size and population abundance (characterising the species ecological optimum) could involve higher resource availability leading to higher individual growth and, consequently, higher populational growth (Schmidt et al., 2004). Experiments have shown that a higher feeding frequency (*i.e.*, higher resource availability) leads to faster cell growth and larger final cell size, but it also leads to an earlier onset of gametogenesis (Be et al., 1981). Thus, if resources are plentiful, then the Be et al. (1981) experiments suggests that individuals should be larger but also mature earlier, which results in shorter generation times and higher local abundance in the sediment (given PF life cycle, Hemleben et al. 1989). This mechanism could explain the expected ecological optimum pattern of large sizes and high abundances. However, it implies that populations in different environments have different generation times, which contradicts the evidence that PF reproduction is synchronised with the lunar periodicity (Bijma et al., 1990a; Jonkers et al., 2015). Moreover, more generations per year at the optimum would result in higher abundance in the sediment, but relative to other populations of the same species, and not relative to the local assemblage (as the usual PF relative abundance data). In the local assemblage, resource availability is the same for all co-occurring species. As smaller species are generally more abundant in the sediment (Fig. 4), relative abundance data regarding the local assemblage potentially blur within-species ecological patterns.

5 Conclusion

Our results caution against using the relative abundance of a species or SST to predict planktonic foraminifera intraspecific shell size variation. Regarding the understanding of PF ecology and evolution, maximum shell size might not indicate that a species is at its ecological optimum, and/or the highest relative abundance of a species in the sediment might not coincide with its ecological optimum. The low predictability of PF intraspecific size variation found in our study also has implications for PF biomass estimation. If shell size is predictable, then more studies are needed to understand what drives the vast majority of the PF within-species size variation. Finally, our results highlight the utility of natural history collections and the importance of studying intraspecific variation when interpreting macroecological patterns.

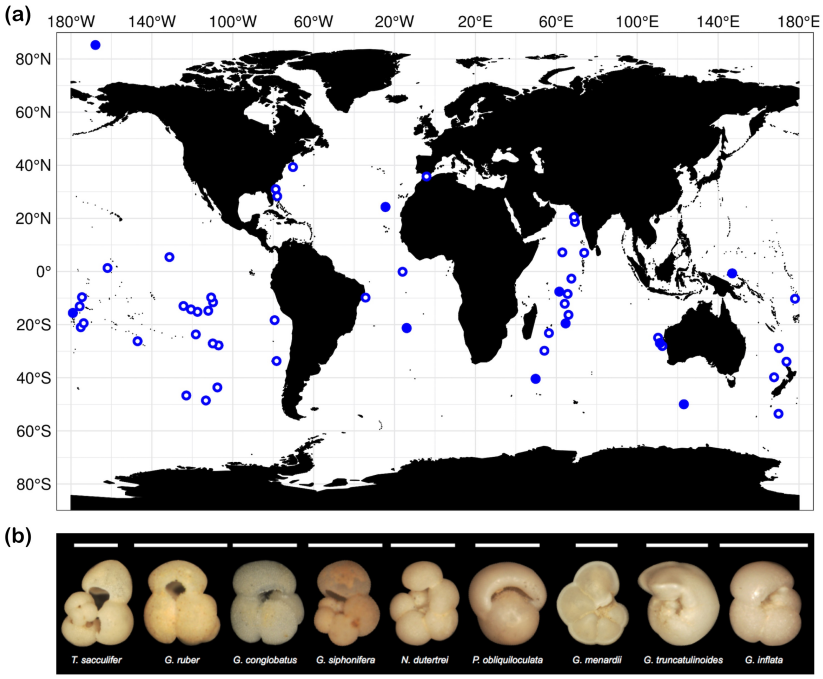

Fig. 1: **(a)** Geographic distribution of the samples used from the Buckley Collection. Each dot on the map includes data on planktonic foraminifera shell size distributions, and corresponding data on relative abundance of species and mean annual values of sea-surface temperature. The filled dots represent the ten samples that were re-sampled to analyse the biases in the Buckley Collection. The sample above 80°N was used just in the collection bias analysis. **(b)** A representative specimen from the Buckley Collection for each species analysed. White bars represent 500 μm (0.5 mm).

Table 1: Overview of the morphometric dataset extracted from the Henry Buckley Collection of Planktonic Foraminifera. Columns: species names; number of individuals measured; number of populations per species (*i.e.*, number of geographical sites, 53 in total); species resolution (*i.e.*, median number of individuals per sample); mounting position in the collection (*i.e.*, position in which the individuals of each species were measured).

Species	**N(ind)**	**N(pop)**	**Resolution**	**Mounting Position**
Trilobatus sacculifer	674	38	15	umbilical or spiral
Globigerinoides ruber	481	39	10	umbilical or spiral
Globigerinoides conglobatus	345	38	8	umbilical
Globigerinella siphonifera	244	37	5	umbilical or spiral
Neogloboquadrina dutertrei	321	30	9	umbilical
Pulleniatina obliquiloculata	295	32	8.5	edge
Globorotalia menardii	665	29	16	umbilical or spiral
Globorotalia truncatulinoides	311	30	8.5	umbilical
Globorotalia inflata	481	20	17.5	umbilical
Total	**3817**	**293**		

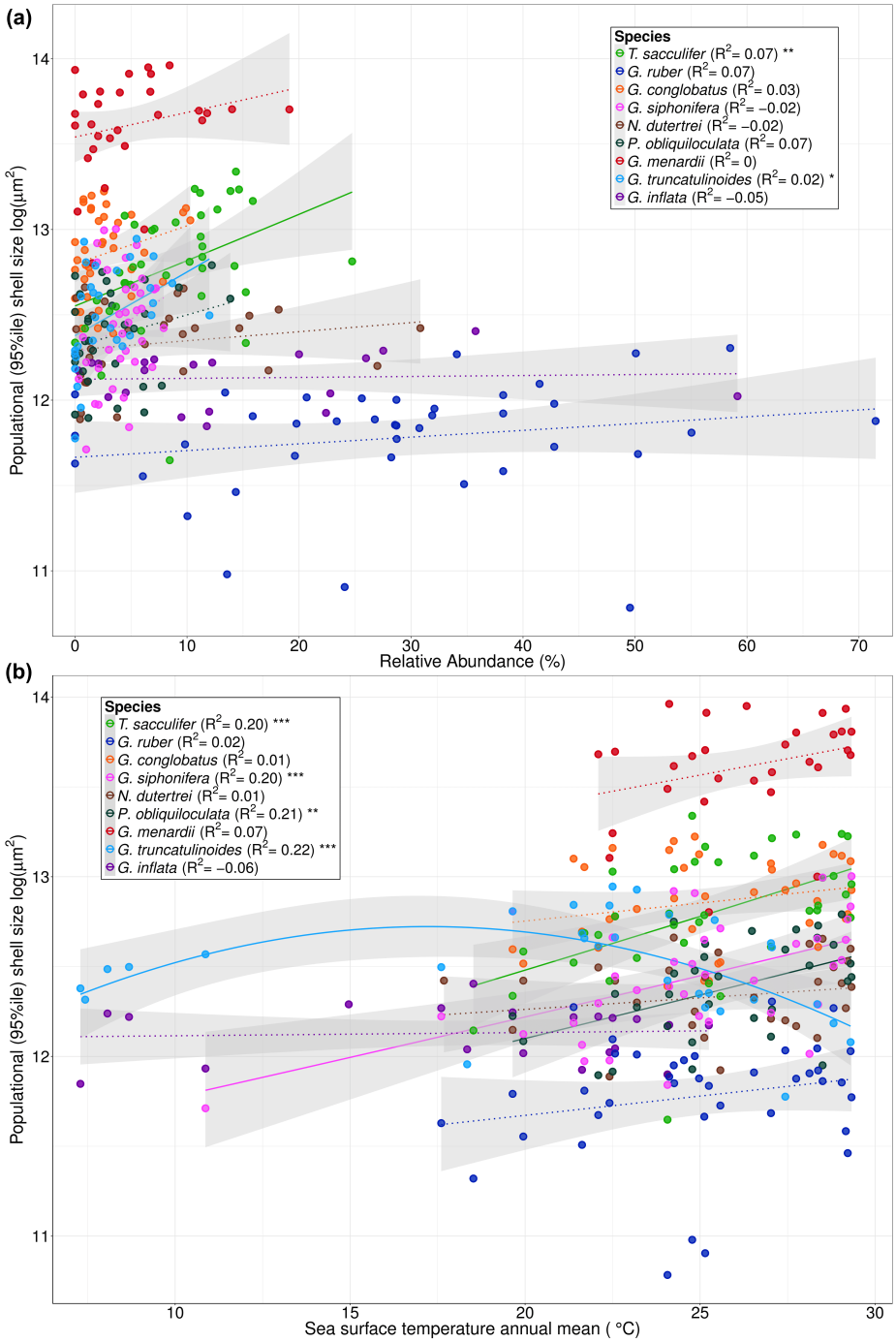

Fig. 2: Relative abundance of species and sea surface temperature do not explain most of the planktonic foraminifera intraspecific size variation. Logarithm of size (represented by the 95th percentile of each population shell size distribution) as a function of **(a)** relative abundance of species and **(b)** mean annual sea surface temperature (SST). The lines represent the generalised linear regression. Solid lines show significant relationship whereas dotted lines non-significant; grey shades show standard error of the model. *G. truncatulinoides* best SST fit was a quadratic function (Table 2). The legend shows the adjusted R^2 for each species. Significance codes: '***' $p<0.001$; '**' $p<0.01$; '*' $p<0.05$; ' ' $p>=0.05$

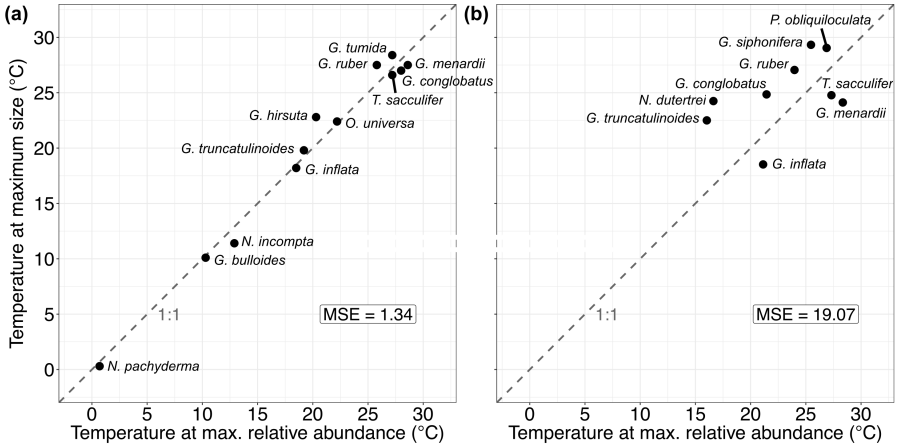

Fig. 3: The sea-surface temperatures at which planktonic foraminifera species reach maximum shell size and maximum relative abundance in the surface sediments. MSE stands for mean squared error with respect to the identity function (1:1 relationship, dashed grey line). **(a)** Data from Schmidt (2002) Table 3.3. **(b)** Data from this study. The current study shows a larger MSE than the one found by Schmidt (2002).

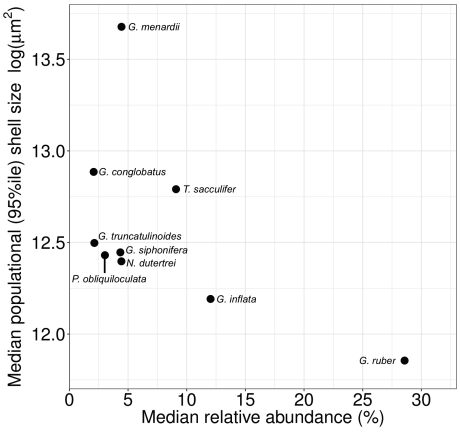

Fig. 4: Relationship between median population shell size (represented by the logarithm of the 95th percentile of each population size distribution) and median relative abundance of each planktonic foraminifera species, within the morphometric dataset. The negative relationship indicates that more abundant species are generally smaller than less abundant ones.

Table 2: Model selection of the generalised linear models (with the Gamma logarithmic error function) testing if planktonic foraminifera shell size (represented by the 95th percentile of each population size distribution) can be predicted by sea surface temperature annual mean (sst) and relative abundance of species (median within 300 km distance) (abund), plus the interaction between these two explanatory variables (sst:abund). Columns: explanatory variables, degrees of freedom, log-likelihood, Akaike Information Criterion corrected for small sample size (AICc), difference in AICc, model weight, adjusted R squared. Explanatory variables in bold indicate best supported model according to model weight.

Explanatory variables	**df**	**logLik**	**AICc**	**ΔAICc**	**weight**	$\mathbf{R^2_{adj}}$
Trilobatus sacculifer						
sst	3	-491.55	989.81	0.00	0.36	0.20
sst^2	4	-490.75	990.72	0.91	0.23	0.22
sst + abund	4	-491.07	991.36	1.55	0.16	0.20
Globigerinoides ruber						
null	2	-470.04	944.42	0.00	0.26	0.00
abund	3	-468.87	944.42	0.01	0.26	0.07
sst	3	-469.18	945.05	0.63	0.19	0.02
Globigerinoides conglobatus						
null	2	-488.93	982.20	0.00	0.22	0.00
abund	3	-487.85	982.41	0.21	0.20	0.03
sst + abund	4	-486.72	982.65	0.45	0.18	0.03
Globigerinella siphonifera						
sst	3	-464.99	936.72	0.00	0.53	0.20
sst + abund	4	-464.84	938.93	2.22	0.18	0.20
sst^2	4	-464.99	939.22	2.50	0.15	0.18
Neogloboquadrina dutertrei						
null	2	-366.22	736.89	0.00	0.36	0.00
sst	3	-365.72	738.35	1.46	0.17	0.01
abund	3	-365.81	738.53	1.64	0.16	-0.02
Pulleniatina obliquiloculata						
sst	3	-393.81	794.47	0.00	0.52	0.21
sst + abund	4	-393.57	796.62	2.15	0.18	0.22
sst^2	4	-393.77	797.03	2.56	0.15	0.19
Globorotalia menardii						
sst^2 + abund + sst^2:abund	5	-391.06	794.72	0.00	0.46	0.16
sst + abund + sst:abund	6	-390.79	797.39	2.67	0.12	0.15
sst	3	-395.33	797.62	2.90	0.11	0.07
Globorotalia truncatulinoides						
sst^2	4	-373.15	755.91	0.00	0.51	0.22
sst^2 + abund	5	-372.80	758.10	2.20	0.17	0.18
sst^2 + abund + sst^2:abund	5	-373.14	758.78	2.88	0.12	0.19
Globorotalia inflata						
null	2	-232.75	470.20	0.00	0.56	0.00
abund	3	-232.70	472.89	2.69	0.15	-0.05
sst	3	-232.74	472.98	2.79	0.14	-0.06

Table 3: Linear mixed-effects models ANOVA, using population size variation as response variable, species as random effects and fixed effects as sea surface temperature annual mean (sst linear effect, sst^2 quadratic effect), relative abundance of species (median within 300 km distance) (abund), plus the interaction between these two explanatory variables (sst:abund). Columns: fixed effects, degrees of freedom, Akaike Information Criterion, log-likelihood, model deviance, chi-squared, p-value, marginal R squared.

Fixed effects	**df**	**AIC**	**logLik**	**dev**	χ^2	**P**	$\mathbf{R}^2_m$
null	8	136.31	-60.15	120.31			0.00
sst	9	130.52	-56.26	112.52	7.79	0.01	0.04
null	9	130.52	-56.26	112.52			0.04
sst^2	10	131.94	-55.97	111.94	0.58	0.45	0.05
null	8	136.31	-60.15	120.31			0.00
abund	9	130.75	-56.38	112.75	7.56	0.01	0.03
sst	9	130.52	-56.26	112.52			0.04
sst + abund	10	124.25	-52.13	104.25	8.27	0.00	0.06
abund	9	130.75	-56.38	112.75			0.03
sst + abund	10	124.25	-52.13	104.25	8.50	0.00	0.06
sst + abund	10	124.25	-52.13	104.25			0.06
sst + abund + sst:abund	11	125.69	-51.85	103.69	0.56	0.45	0.06

Acknowledgements We gratefully acknowledge Andy Purvis and Isabel S. Fenton for insightful discussions throughout the project. We also thank Anieke Brombacher for patient assistance with the Image-Pro Premier software and, together with Mauro T. C. Sugawara, for helpful comments in earlier versions of the manuscript.

Authors contribution: MCR designed the research question, with input from MK. MCR imaged and measured all the individuals, with input from GM. MCR and THGE designed the statistical analysis. MCR performed the analysis and wrote the initial draft. All authors reviewed and edited the manuscript. The authors declare no conflict of interest.

Funding: MCR is funded by the Graduate School of the National Oceanography Centre Southampton and DAAD Research Grants for Doctoral Candidates 2016/17 (57210260). THGE is funded by NERC Advanced Research Fellowship NE/J018163/1.

References

Aldridge D, Beer C, Purdie D (2012) Calcification in the planktonic foraminifera globigerina bulloides linked to phosphate concentrations in surface waters of the north atlantic ocean. Biogeosciences 9(5):1725–1739

Amante C, Eakins BW (2009) ETOPO1 1 Arc-Minute Global Relief Model: procedures, data sources and analysis. NOAA Technical Memorandum NESDIS NGDC-24. National Geophysical Data Center, NOAA.

Anderson OR, Be AW (1976) A cytochemical fine structure study of phagotrophy in a planktonic foraminifer, *Hastigerina pelagica* (d'Orbigny). The Biological Bulletin 151(3):437–449

Andre A, Weiner A, Quillevere F, Aurahs R, Morard R, Douady CJ, de Garidel-Thoron T, Escarguel G, De Vargas C, Kucera M (2013) The cryptic and the apparent reversed: lack of genetic differentiation within the morphologically diverse plexus of the planktonic foraminifer *Globigerinoides sacculifer*. Paleobiology 39(1):21–39

Aurahs R, Treis Y, Darling K, Kucera M (2011) A revised taxonomic and phylogenetic concept for the planktonic foraminifer species globigerinoides ruber based on molecular and morphometric evidence. Marine Micropaleontology 79(1-2):1–14

Barton AD, Pershing AJ, Litchman E, Record NR, Edwards KF, Finkel ZV, Kiørboe T, Ward BA (2013) The biogeography of marine plankton traits. Ecology Letters 16(4):522–534

Barton K (2017) MuMIn: Multi-Model Inference. URL https://CRAN.R-project.org/package=MuMIn, R package version 1.40.0

Bates D, Machler M, Bolker B, Walker S (2015) Fitting linear mixed-effects models using *lme4*. Journal of Statistical Software 67(1):1–48

Be AWH, Anderson OR (1976) Gametogenesis in planktonic foraminifera. Science 192(4242):890–892

Be AWH, Hutson WH (1977) Ecology of planktonic foraminifera and biogeographic patterns of life and fossil assemblages in the Indian Ocean. Micropaleontology 23(4):369–414

Be AWH, Harrison SM, Lott L (1973) *Orbulina universa* d'Orbigny in the Indian Ocean. Micropaleontology 19(2):150–192

Be AWH, Caron DA, Anderson OR (1981) Effects of feeding frequency on life processes of the planktonic foraminifer *Globigerinoides sacculifer* in laboratory culture. Journal of the Marine Biological Association of the United Kingdom 61(1):257–277

Beer CJ, Schiebel R, Wilson PA (2010) Testing planktic foraminiferal shell weight as a surface water [CO_3^{2-}] proxy using plankton net samples. Geology 38(2):103–106

Berger WH, Piper DJ (1972) Planktonic foraminifera: differential settling, dissolution, and redeposition. Limnology and Oceanography 17(2):275–287

Berlow EL, Dunne JA, Martinez ND, Stark PB, Williams RJ, Brose U (2009) Simple prediction of interaction strengths in complex food webs. Proceedings of the National Academy of Sciences 106(1):187–191

Bijma J, Erez J, Hemleben C (1990a) Lunar and semi-lunar reproductive cycles in some spinose planktonic foraminifers. Journal of Foraminiferal Research 20(2):117–127

Bijma J, Faber WW, Hemleben C (1990b) Temperature and salinity limits for growth and survival of some planktonic foraminifers in laboratory cultures. Journal of Foraminiferal Research 20(2):95–116

Bijma J, Hemleben C, Oberhaensli H, Spindler M (1992) The effects of increased water fertility on tropical spinose planktonic foraminifers in laboratory cultures. Journal of Foraminiferal Research 22(3):242–256

Bolnick DI, Amarasekare P, Araujo MS, Burger R, Levine JM, Novak M, Rudolf VH, Schreiber SJ, Urban MC, Vasseur DA (2011) Why intraspecific trait variation matters in community ecology. Trends in Ecology & Evolution 26(4):183–192

Boyce DG, Frank KT, Leggett WC (2015) From mice to elephants: overturning the 'one size fits all' paradigm in marine plankton food chains. Ecology Letters 18(6):504–515

Brombacher A, Elder LE, Hull PM, Wilson PA, Ezard TH (2018) Calibration of test diameter and area as proxies for body size in the planktonic foraminifer *Globoconella Puncticulata*. Journal of Foraminiferal Research 48(3):241–245

Brown JH, Gillooly JF, Allen AP, Savage VM, West GB (2004) Toward a metabolic theory of ecology. Ecology 85(7):1771–1789

Caron DA, Be AW, Anderson OR (1981) Effects of variations in light intensity on life processes of the planktonic foraminifer *Globigerinoides sacculifer* in laboratory culture. Journal of the Marine Biological Association of the United Kingdom 62(2):435–451

Caron DA, Faber WW, Be AWH (1987a) Effects of temperature and salinity on the growth and survival of the planktonic foraminifer *Globigerinoides sacculifer*. Journal of the Marine Biological Association of the United Kingdom 67(2):323–341

Caron DA, Faber WW, Be AWH (1987b) Growth of the spinose planktonic foraminifer *Orbulina universa* in laboratory culture and the effect of temperature on life processes. Journal of the Marine Biological Association of the United Kingdom 67(2):343–358

Damuth J (1981) Population density and body size in mammals. Nature 290(5808):699 – 700

Darling KF, Wade CM (2008) The genetic diversity of planktic foraminifera and the global distribution of ribosomal rna genotypes. Marine Micropaleontology 67(3):216–238

De Vargas C, Zaninetti L, Hilbrecht H, Pawlowski J (1997) Phylogeny and rates of molecular evolution of planktonic foraminifera: SSU rDNA sequences compared to the fossil record. Journal of Molecular Evolution 45(3):285–294

De Vargas C, Norris R, Zaninetti L, Gibb SW, Pawlowski J (1999) Molecular evidence of cryptic speciation in planktonic foraminifers and their relation to oceanic provinces. Proceedings of the National Academy of Sciences 96(6):2864–2868

Des Roches S, Post DM, Turley NE, Bailey JK, Hendry AP, Kinnison MT, Schweitzer JA, Palkovacs EP (2018) The ecological importance of intraspecific variation. Nature Ecology & Evolution 2(1):57

Emmerson MC, Raffaelli D (2004) Predator–prey body size, interaction strength and the stability of a real food web. Journal of Animal Ecology 73(3):399–409

Ezard TH, Aze T, Pearson PN, Purvis A (2011) Interplay between changing climate and species' ecology drives macroevolutionary dynamics. Science 332(6027):349–351

Fenchel T (1974) Intrinsic rate of natural increase: the relationship with body size. Oecologia 14(4):317–326

Fenton IS, Pearson PN, Jones TD, Purvis A (2016) Environmental predictors of diversity in recent planktonic foraminifera as recorded in marine sediments. PLoS One 11(11):e0165522

Gianuca AT, Pantel JH, De Meester L (2016) Disentangling the effect of body size and phylogenetic distances on zooplankton top-down control of algae. Proceedings of the Royal Society of London B: Biological Sciences 283(1828):20160487

Hart SP, Schreiber SJ, Levine JM (2016) How variation between individuals affects species coexistence. Ecology Letters 19(8):825–838

Hecht AD (1976) An ecologic model for test size variation in Recent planktonic foraminifera; applications to the fossil record. The Journal of Foraminiferal Research 6(4):295–311

Hemleben C, Spindler M, Breitinger I, Ott R (1987) Morphological and physiological responses of *Globigerinoides sacculifer* (Brady) under varying laboratory conditions. Marine Micropaleontology 12:305–324

Hemleben C, Spindler M, Anderson OR (1989) Modern planktonic foraminifera, 1st edn. Springer-Verlag New York Inc.

Hijmans RJ (2015) geosphere: Spherical Trigonometry. URL https://CRAN.R-project.org/package=geosphere, R package version 1.5-1

Huete-Ortega M, Cermeno P, Calvo-Diaz A, Maranon E (2012) Isometric size-scaling of metabolic rate and the size abundance distribution of phytoplankton. Proceedings of the Royal Society of London B: Biological Sciences 279(1734):1815–1823

Jennings S, Mackinson S (2003) Abundance–body mass relationships in size-structured food webs. Ecology Letters 6(11):971–974

Jonkers L, Kucera M (2015) Global analysis of seasonality in the shell flux of extant planktonic foraminifera. Biogeosciences 12(7):2207–2226

Jonkers L, Reynolds CE, Richey J, Hall IR (2015) Lunar periodicity in the shell flux of planktonic foraminifera in the Gulf of Mexico. Biogeosciences 12(10):3061–3070

Kahn MI (1981) Ecological and paleoecological implications of the phenotypic variation in three species of living planktonic foraminifera from the northeastern Pacific Ocean (50°N, 145°W). Journal of Foraminiferal Research 11(3):203–211

Kennett JP (1976) Phenotypic variation in some Recent and late Cenozoic planktonic foraminifera (in Foraminifera II), vol 2, 1st edn, Academic Press New York, pp 111–169

Kirkpatrick M, Barton NH (1997) Evolution of a species' range. The American Naturalist 150(1):1–23

Kucera M (2007) Planktonic foraminifera as tracers of past oceanic environments (in Developments in Marine Geology), vol 1, 1st edn, Elsevier, chap 6, pp 213–262

Liancourt P, Callaway RM, Michalet R (2005) Stress tolerance and competitive-response ability determine the outcome of biotic interactions. Ecology 86(6):1611–1618

Litchman E, Ohman MD, Kiørboe T (2013) Trait-based approaches to zooplankton communities. Journal of Plankton Research 35(3):473–484

Locarnini RA, Mishonov AV, Antonov JI, Boyer TP, Garcia HE, Baranova OK, Zweng MM, Paver CR, Reagan JR, Johnson DR, Hamilton M, Seidov D (2013) World Ocean Atlas 2013, Volume 1: Temperature. NOAA Atlas NESDIS 73:1–40

Malmgren B, Kennett JP (1976) Biometric analysis of phenotypic variation in Recent *Globigerina bulloides* d'Orbigny in the southern Indian Ocean. Marine Micropaleontology

1:3–25
Malmgren BA, Kennett JP (1977) Biometric differentiation between Recent *Globigerina bulloides* and *Globigerina falconensis* in the southern Indian Ocean. The Journal of Foraminiferal Research 7(2):131–148
Moller T, Schulz H, Kucera M (2013) The effect of sea surface properties on shell morphology and size of the planktonic foraminifer *Neogloboquadrina pachyderma* in the North Atlantic. Palaeogeography, Palaeoclimatology, Palaeoecology 391:34–48
Morard R, Quillevere F, Douady CJ, de Vargas C, de Garidel-Thoron T, Escarguel G (2011) Worldwide genotyping in the planktonic foraminifer globoconella inflata: implications for life history and paleoceanography. PLoS One 6(10):e26665
Morard R, Garet-Delmas MJ, Mahe F, Romac S, Poulain J, Kucera M, Vargas C (2018) Surface ocean metabarcoding confirms limited diversity in planktonic foraminifera but reveals unknown hyper-abundant lineages. Scientific Reports 8(1):2539
Morey AE, Mix AC, Pisias NG (2005) Planktonic foraminiferal assemblages preserved in surface sediments correspond to multiple environment variables. Quaternary Science Reviews 24(7-9):925–950
Mousing EA, Ribeiro S, Chisholm C, Kuijpers A, Moros M, Ellegaard M (2017) Size differences of Arctic marine protists between two climate periods–using the paleoecological record to assess the importance of within-species trait variation. Ecology and Evolution 7(1):3–13
Muller H, Geller W (1993) Maximum growth rates of aquatic ciliated protozoa: the dependence on body size and temperature reconsidered. Archiv fur Hydrobiologie 126:315–327
Orr HA (2009) Fitness and its role in evolutionary genetics. Nature Reviews Genetics 10(8):531
Pante E, Simon-Bouhet B (2013) *marmap*: a package for importing, plotting and analyzing bathymetric and topographic data in R. PLoS One 8(9):e73051
Petchey OL, Beckerman AP, Riede JO, Warren PH (2008) Size, foraging, and food web structure. Proceedings of the National Academy of Sciences 105(11):4191–4196
Peters RH, Wassenberg K (1983) The effect of body size on animal abundance. Oecologia 60(1):89–96
Quillevere F, Morard R, Escarguel G, Douady CJ, Ujiie Y, de Garidel-Thoron T, De Vargas C (2013) Global scale same-specimen morpho-genetic analysis of *Truncorotalia truncatulinoides*: A perspective on the morphological species concept in planktonic foraminifera. Palaeogeography, Palaeoclimatology, Palaeoecology 391:2–12
Rehfeldt GE, Leites LP, Joyce DG, Weiskittel AR (2018) Role of population genetics in guiding ecological responses to climate. Global Change Biology 24(2):858–868
Reuman DC, Mulder C, Raffaelli D, Cohen JE (2008) Three allometric relations of population density to body mass: theoretical integration and empirical tests in 149 food webs. Ecology Letters 11(11):1216–1228
Rillo MC, Whittaker J, Ezard THG, Purvis A, Henderson AS, Stukins S, Miller CG (2016) The unknown planktonic foraminiferal pioneer Henry A. Buckley and his collection at the Natural History Museum, London. Journal of Micropalaeontology 36(2):191–194
Rillo MC, Kucera M, Ezard THG, Miller CG (2018) (preprint) Surface sediment samples from early age of seafloor exploration can provide a late 19th century baseline of the marine environment. bioRxiv DOI https://doi.org/10.1101/419770
Rutherford S, D'Hondt S, Prell W (1999) Environmental controls on the geographic distribution of zooplankton diversity. Nature 400(6746):749
Sagarin RD, Gaines SD (2002) The 'abundant centre' distribution: to what extent is it a biogeographical rule? Ecology Letters 5(1):137–147

Savage VM, Gillooly JF, Brown JH, West GB, Charnov EL (2004) Effects of body size and temperature on population growth. The American Naturalist 163(3):429–441

Schmidt DN (2002) Size variability in planktic foraminifers. PhD thesis, ETH Zurich, https://doi.org/10.3929/ethz-a-004353260

Schmidt DN, Renaud S, Bollmann J, Schiebel R, Thierstein HR (2004) Size distribution of Holocene planktic foraminifer assemblages: biogeography, ecology and adaptation. Marine Micropaleontology 50(3):319–338

Schmidt DN, Lazarus D, Young JR, Kucera M (2006) Biogeography and evolution of body size in marine plankton. Earth-Science Reviews 78(3-4):239–266

Seears HA, Darling KF, Wade CM (2012) Ecological partitioning and diversity in tropical planktonic foraminifera. BMC Evolutionary Biology 12(1):54

Siccha M, Kucera M (2017) ForCenS, a curated database of planktonic foraminifera census counts in marine surface sediment samples. Scientific Data 4:170109

Sommer U, Peter KH, Genitsaris S, Moustaka-Gouni M (2017) Do marine phytoplankton follow Bergmann's rule *sensu lato*? Biological Reviews 92(2):1011–1026

Tittensor DP, Mora C, Jetz W, Lotze HK, Ricard D, Berghe EV, Worm B (2010) Global patterns and predictors of marine biodiversity across taxa. Nature 466(7310):1098

Ujiie Y, Asami T, de Garidel-Thoron T, Liu H, Ishitani Y, de Vargas C (2012) Longitudinal differentiation among pelagic populations in a planktic foraminifer. Ecology and Evolution 2(7):1725–1737

Van Sebille E, Scussolini P, Durgadoo JV, Peeters FJ, Biastoch A, Weijer W, Turney C, Paris CB, Zahn R (2015) Ocean currents generate large footprints in marine palaeoclimate proxies. Nature Communications 6:6521

Villarino E, Watson JR, Jonsson B, Gasol JM, Salazar G, Acinas SG, Estrada M, Massana R, Logares R, Giner CR, et al. (2018) Large-scale ocean connectivity and planktonic body size. Nature Communications 9(1):142

Violle C, Enquist BJ, McGill BJ, Jiang L, Albert CH, Hulshof C, Jung V, Messier J (2012) The return of the variance: intraspecific variability in community ecology. Trends in Ecology & Evolution 27(4):244–252

Wang Y, Chu C, Maestre FT, Wang G (2008) On the relevance of facilitation in alpine meadow communities: an experimental assessment with multiple species differing in their ecological optimum. Acta Oecologica 33(1):108–113

Weiner AK, Weinkauf MF, Kurasawa A, Darling KF, Kucera M, Grimm GW (2014) Phylogeography of the tropical planktonic foraminifera lineage *Globigerinella* reveals isolation inconsistent with passive dispersal by ocean currents. PLoS One 9(3):e92148

Weinkauf MF, Kunze JG, Waniek JJ, Kucera M (2016) Seasonal variation in shell calcification of planktonic foraminifera in the NE Atlantic reveals species-specific response to temperature, productivity, and optimum growth conditions. PLoS One 11(2):e0148363

White EP, Ernest SM, Kerkhoff AJ, Enquist BJ (2007) Relationships between body size and abundance in ecology. Trends in Ecology & Evolution 22(6):323–330

Woodward G, Ebenman B, Emmerson M, Montoya JM, Olesen JM, Valido A, Warren PH (2005) Body size in ecological networks. Trends in Ecology & Evolution 20(7):402–409

Yvon-Durocher G, Reiss J, Blanchard J, Ebenman B, Perkins DM, Reuman DC, Thierry A, Woodward G, Petchey OL (2011) Across ecosystem comparisons of size structure: methods, approaches and prospects. Oikos 120(4):550–563

Zhang D (2017) A coefficient of determination for generalized linear models. The American Statistician 71(4):310–316

Supplementary Information

S1 Expeditions

Table S1: Information about the samples from the Henry Buckley Collection of Planktonic Foraminifera at The Natural History Museum, London (NHMUK) used in our morphometric analysis. Columns: NHMUK Internal Record Number of the sediment in the Ocean-Bottom Deposits Collection (OBD IRN); name of the Vessel that collected the sample; Year the sample was collected; latitude (Lat) and longitude (Long) given in decimal degrees; sea surface temperature (SST) in Celsius degrees; water Depth in meters; Sampling method used in the historical expedition (extracted from OBD Collection metadata); depth below the sea floor (Dbsf) sampled in centimetres; number of individuals, N(ind), and species, N(ssp), measured at each site.

OBD IRN	Vessel	Year	Lat	Long	SST	Depth(m)	Sampling	Dbsf(cm)	N(ind)	N(ssp)
31945	CS *Britannia*	1899	39.21	-70.24	19.25	-2731	Sounding	surface	65	1
34297	CS *Buccaneer*	1886	-0.03	-15.94	26.30	-3226	Sounding	surface	57	1
30724	HEMS *Mabahiss*	1934	7.19	63.04	28.38	-4346	Core	4-5.5	53	7
35818	HMIMS *Investigator*	1906	20.44	68.84	27.24	-2680	Sounding	surface	56	5
17229	HMNZS *Lachlan*	1955	-33.88	173.83	17.80	-2464	Worsel sampler	surface	106	8
17262	HMNZS *Pukaki*	1957	-53.63	169.87	7.95	-746	Dietz grab	surface	52	2
33286	HMS *Challenger*	1873	24.33	-24.47	23.16	-5153	Sounding	surface	46	1
32657	HMS *Challenger*	1874	-50.02	123.07	9.32	-3976	Sounding	surface	11	1
33668	HMS *Challenger*	1875	-0.70	147.00	29.40	-2213	Sounding	surface	95	7
34607	HMS *Challenger*	1875	-33.70	-78.30	16.79	-3798	Sounding	surface	8	1
34991	HMS *Challenger*	1876	-21.25	-14.03	23.61	-3740	Dredge	surface	181	8
34671	HMS *Egeria*	1887	-19.57	64.63	24.83	-2708	Sounding	surface	66	8
34676	HMS *Egeria*	1887	-23.23	56.30	25.14	-4646	Sounding	surface	73	9
34678	HMS *Egeria*	1887	-29.93	54.10	21.13	-4211	Sounding	surface	63	8
34993	HMS *Egeria*	1889	-15.65	-179.06	28.05	-2519	Sounding	surface	124	8
35238	HMS *Egeria*	1894	7.08	73.80	28.57	-2658	Sounding	surface	66	7
16621	HMS *Enterprise*	1962	30.90	-78.68	26.63	-821	Dredge	surface	35	1
36043	HMS *Penguin*	1891	-28.01	112.46	21.94	-1206	Sounding	surface	189	9
36053	HMS *Penguin*	1891	-26.94	111.18	22.66	-3350	Sounding	surface	203	9
36057	HMS *Penguin*	1891	-24.89	110.39	22.83	-3829	Sounding	surface	193	9
36361	HMS *Penguin*	1896	-10.21	178.01	28.91	-4844	Sounding	surface	123	8
36515	HMS *Penguin*	1897	-9.68	-174.62	28.05	-4057	Sounding	surface	71	6
36683	HMS *Penguin*	1897	1.21	-161.84	27.32	-4634	Sounding	surface	47	8
36704	HMS *Penguin*	1897	-13.17	-175.69	28.05	-3952	Sounding	surface	111	7
37130	HMS *Sealark*	1905	-8.42	65.63	28.35	-3694	Sounding	surface	78	7
37148	HMS *Sealark*	1905	-7.59	61.48	28.06	-3507	Sounding	surface	87	8
37149	HMS *Sealark*	1905	-2.70	67.38	28.95	-3594	Sounding	surface	119	7
37190	HMS *Sealark*	1905	-12.12	64.12	27.16	-3322	Sounding	surface	72	7
37299	HMS *Serpent*	1868	18.63	69.17	27.85	-3261	Sounding	surface	9	1
38482	HMS *Waterwitch*	1895	-40.45	49.82	7.78	-3780	Sounding	surface	39	2
17031	RNZFA *Tui*	1956	-39.77	167.75	16.04	-1137	Dietz grab	surface	71	4
17240	RNZFA *Tui*	1956	-28.88	170.00	22.18	-3021	Dietz grab	surface	165	8
17273	RNZFA *Tui*	1958	-20.95	-175.23	25.66	-869	Cone dredge	surface	40	6
16657	RV *Argo*	1960	-16.42	66.03	26.20	-2810	Core	4-9	60	8
16365	RV *Horizon*	1953	-19.48	-173.73	25.66	-4347	Gravity core	5-10	43	4
16640	RV *Horizon*	1953	-13.09	-124.28	26.67	-3456	Gravity core	4-8	58	7
16641	RV *Horizon*	1953	-14.27	-120.68	25.97	-3617	Gravity core	4-8	41	6
16642	RV *Horizon*	1953	-15.22	-117.51	25.97	-3641	Gravity core	1-4	32	5
16656	RV *Horizon*	1958	-23.61	-118.22	23.98	-3362	Gravity core	7-11	48	5
(1971,O87)	RV *Maria Paolina G*	1970	35.68	-4.08	18.17	-1500	Sphincter core	0-5	40	3
16645	RV *Spencer F. Baird*	1957	5.43	-131.32	27.65	-3415	Gravity core	7-10	51	6
16646	RV *Spencer F. Baird*	1957	-26.32	-147.12	21.85	-2312	Gravity core	3-7	54	6
16647	RV *Spencer F. Baird*	1957	-46.75	-123.00	9.91	-4030	Gravity core	6-11	53	2
16648	RV *Spencer F. Baird*	1957	-48.48	-113.28	8.06	-2677	Gravity core	0-8	41	2
16649	RV *Spencer F. Baird*	1957	-43.72	-107.60	10.99	-3141	Gravity core	3-7	17	3
16370	RV *Spencer F. Baird*	1958	-11.70	-109.72	25.27	-3296	Gravity core	0-3	1	1
16650	RV *Spencer F. Baird*	1958	-18.33	-79.34	20.07	-3157	Gravity core	8-12	49	7
16651	RV *Spencer F. Baird*	1958	-27.93	-106.92	21.45	-3039	Gravity core	8-15	67	6
16652	RV *Spencer F. Baird*	1958	-27.15	-109.83	21.45	-2819	Gravity core	10-14	51	5
16653	RV *Spencer F. Baird*	1958	-14.73	-112.10	24.90	-3034	Gravity core	12-15	69	7
16654	RV *Spencer F. Baird*	1958	-9.88	-110.68	25.26	-2712	Gravity core	5-9	46	7
17162	RV *Vema*	1959	28.40	-77.93	24.89	-1004	Piston core	0-2	136	8
17359	RV *Vema*	1959	-9.75	-34.40	27.14	-4123	Piston core	5-6	86	6

S2 Species list and shell area histograms

Modern species
Beella digitata
Berggrenia pumilio
Candeina nitida
Globigerina bulloides
Globigerina falconensis
Globigerinella adamsi
Globigerinella calida
Globigerinella siphonifera
Globigerinita glutinata
Globigerinoides conglobatus
Globigerinoides ruber
Globoquadrina conglomerata
Globorotalia crassaformis
Globorotalia hirsuta
Globorotalia inflata
Globorotalia menardii
Globorotalia scitula
Globorotalia truncatulinoides
Globorotalia tumida
Globorotaloides hexagonus
Globoturborotalita rubescens
Globoturborotalita tenella
Hastigerina pelagica
Neogloboquadrina dutertrei
Neogloboquadrina pachyderma
Orbulina universa
Pulleniatina obliquiloculata
Sphaeroidinella dehiscens
Tenuitella iota
Trilobatus sacculifer
Turborotalita humilis
Turborotalita quinqueloba

Table S2: List of all species present in the sea-floor sediment samples of the Buckley Collection selected to amass our morphometric dataset. Only extant species are present in these samples. Species and genus names were updated to their modern names.

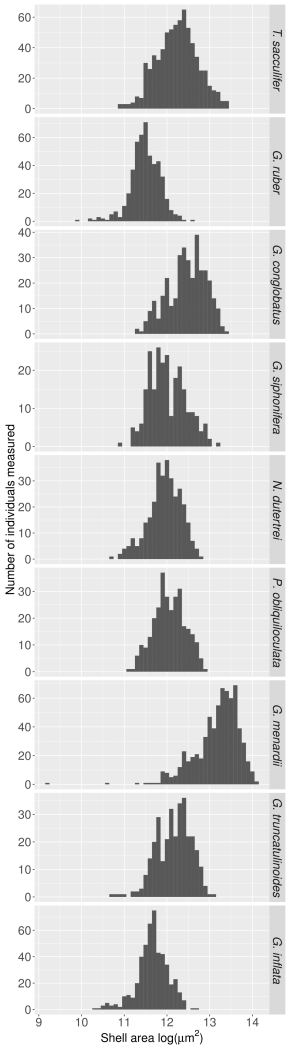

Fig. S1: Shell area histograms for each of the nine species in our planktonic foraminifera size dataset. Total of 3817 individuals measured. See also Table 1.

S3 Museum collection shell size bias analysis

The Buckley Collection could have a collector effort bias towards larger (or smaller) specimens, resulting in distorted shell size distributions. To assess this bias, we re-sampled ten original bulk sediments of the NHMUK Ocean-Bottom Deposits Collection (OBD) Collection, from which the Buckley Collection was created (Fig. 1a, Table SI S3). Samples were chosen to encompass different oceans, latitudes and marine expeditions; however, the final choice also depended on the availability of bulk sediment samples in the OBD Collection.

Half of the amount available in the OBD containers was further split into two equal parts, leaving an archive sample and a sample to be processed. The sample processing consisted of weighing, wet washing over a 63μm sieve and drying in a 60°C oven. The residues were further dry sieved over a 150μm sieve and the coarser fraction was split with a microsplitter as many times as needed to produce a representative aliquot containing around 300 PF shells. All PF specimens in each of the nine final splits were identified by MCR and MK under a stereomicroscope to species level, resulting in a total of 2,611 individuals belonging to 31 species (see also Rillo et al. 2018). This way, we calculated the relative abundance of each species in each sample.

We then mounted species-specific slides from the re-sampled samples and extracted shell size data in the same way as for the slides of the Buckley Collection (section 2.2). Only species also present in the Buckley Collection samples were measured, resulting in 1824 specimens from 20 species (Table SI S3). For each species in each sample, we log-transformed its population shell size distribution and calculated the mean, median, 75th percentile, 95th percentile and maximum value of each distribution. We then regressed each of these five metrics of the Buckley Collection against the re-sampled data and calculated the mean squared error with respect to the identity function (1:1 relationship). This comparison included 65 populations from 2873 individuals (1824 from the re-sampled samples and 1049 from the Buckley Collection samples), all collected in the ten sites (Fig. 1a, Table SI S3). The mean squared error was lowest for the 95th percentile (Fig. SI S2), meaning that this metric is the least biased measurement of the Buckley Collection when considering log-transformed shell area.

Table S3: Information about the samples re-sampled from the Ocean Bottom Deposits Collection at The Natural History Museum, London (NHMUK) used in our museum collection size bias analysis. Columns: NHMUK Internal Record Number of the sediment in the Ocean-Bottom Deposits Collection (OBD IRN); name of the Vessel that collected the sample; latitude (Lat) and longitude (Long) given in decimal degrees; water depth in meters; sampled mass in grams; number of times washed sediment was split, N(splits), until around 300 individuals; number of planktonic foraminifera specimens, N(ind), and species, N(ssp), measured in each re-sampled sample. For more information, see Table SI S1.

OBD IRN	Vessel	Lat	Long	Depth (m)	Mass (g)	N(splits)	N(ind)	N(ssp)
32657	HMS *Challenger*	-50.02	123.07	-3976	0.19	5	14	1
34991	HMS *Challenger*	-21.25	-14.03	-3740	9.35	7	239	11
33668	HMS *Challenger*	-0.70	147.00	-2213	1.98	7	185	7
33286	HMS *Challenger*	24.33	-24.47	-5153	2.73	5	31	3
34671	HMS *Egeria*	-19.57	64.63	-2708	1.23	5	348	11
34993	HMS *Egeria*	-15.65	-179.06	-2519	2.42	8	262	8
36053	HMS *Penguin*	-26.94	111.18	-3350	1.49	5	230	10
37148	HMS *Sealark*	-7.59	61.48	-3507	2.86	8	222	11
38482	HMS *Waterwitch*	-40.45	49.82	-3780	1.51	6	67	2
14609	*Alpha 6*	85.25	-167.90	-1774	0.57	4	226	1
						TOTAL	1824	20

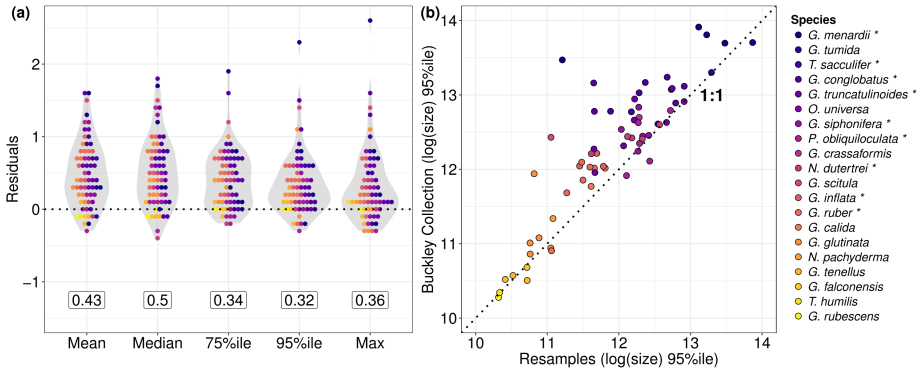

Fig. S2: Difference in shell size distributions between populations of the re-sampled samples and the Buckley Collection samples. Species are coloured and ordered by shell size (larger sizes in purple-blue, smaller sizes in orange-yellow); species marked with (∗) were present in our worldwide morphometric dataset. **(a)** Residuals were calculated between the Buckley Collection and the re-sampled samples with respect to the identity function (1:1 relationship), using log-transformed population shell sizes. Numbers indicate mean squared error (MSE). **(b)** Plot of the 95th percentile of the log-transformed population shell size distributions from the Buckley Collection against the re-sampled samples, line 1:1 represents the identity function.

S3.1 Linear mixed-effects regression using the re-sampled populations (bias analysis)

Using the re-sampled data described above, we tested whether relative abundance variation significantly explains population shell size variation. Since the re-sampled data includes only ten samples (Fig. 1a), there were not enough populations within each species to use

species-specific GLM. Instead, we used linear mixed-effect models. The log-transformed 95th percentile of the population shell size distributions was modelled as the response variable, and the independent fixed effect was the local relative abundance (median within 300 km distance). Species were modelled as random effects, allowing for random intercepts and slopes (*i.e.*, the intercept and slope of the relationship between shell size and the relative abundance may vary among species). We used the Likelihood Ratio Test (LRT) to compare the likelihood of the fixed effect. We calculated the LRT between the models with and without the effect. Significance of each fixed effect was given through the LRT. Marginal R^2 (R^2_m), which is associated with the fixed effects, was calculated for each LMER model (Barton, 2017).

Table S4: Linear mixed-effects models ANOVA, using population size variation as response variable, species as random effects (r.e.) and either a null model (H0) or relative abundance (H1) as explanatory variable. Columns: model explanatory variables (fixed effects), degrees of freedom, Akaike Information Criterion, log-likelihood, model deviance, chi-squared, p-value, marginal R squared.

Explanatory variables	**df**	**AIC**	**logLik**	**dev**	χ^2	**P**	$\mathbf{R^2_m}$
H0: 1 + r.e.	5	130.20	-60.10	120.20			0.00
H1: (abund) + r.e.	6	130.02	-59.01	118.02	2.18	0.14	0.07

S4 Dissolution results

We carried out a linear-mixed effect model (LMER) using the log-transformed 95th percentile of the population shell size as the response variable, and each sample's water depth as the independent fixed variable (effect) (see depths in Table SI S1. Species were modelled as random effects, allowing for random intercepts and slopes, which takes into account interspecific variation on resistance to dissolution. We used LRT to test for significance of the fixed effect. If dissolution affected our results, we would expect water depth to significantly explain part of the population shell size variation we found. However, the LMER results show that water depth is not a significant explanatory variable of PF population shell size variation in our dataset (p-value > 0.05, Table SI S5).

Table S5: Linear mixed-effects models ANOVA, using population size variation as response variable, species as random effects and either a null model (H0) or water depth (H1) as explanatory variable. Columns: model explanatory variables (fixed effects), degrees of freedom, Akaike Information Criterion, log-likelihood, model deviance, chi-squared, p-value, marginal R squared.

Explanatory variables	**df**	**AIC**	**logLik**	**dev**	χ^2	**P**	$\mathbf{R^2_m}$
H0: 1 + r.e.	5	151.19	-70.60	141.19			0.00
H1: (water depth) + r.e.	6	151.36	-69.68	139.36	1.83	0.18	0.00

S5 Nearest neighbour results

We ran the same generalised linear models (GLM) analysis as described in section 2, but using the species relative abundance retrieved from the nearest neighbouring sample of the ForCenS database (instead of the median relative abundance of the samples within 300 km distance). Although the order of the best-supported models changed for some species, the models weights and the ΔAICc are still consistent when compared to the model using the median relative abundance within 300 km radius (Table 2). One example is *G. ruber*: here the best supported model is the abundance one (Table SI S6) whereas for the median relative abundance within 300 km the best supported model is the null model (abund, Table 2). However, the ΔAICc between these two models of *G. ruber* is close to zero (0.02) as well as the difference in the models weights (0.01), consistent with Table 2.

Table S6: Model selection of the generalised linear models (with the Gamma logarithmic error function) testing if planktonic foraminifera shell size (represented by the 95th percentile of each population size distribution) can be predicted by sea surface temperature annual mean (sst) and relative abundance of species (nearest neighbouring ForCenS sample) (abund), plus the interaction between these two explanatory variables (sst:abund). Columns: explanatory variables, degrees of freedom, log-likelihood, Akaike Information Criterion corrected for small sample size, difference in AICc, model weight, adjusted R squared.

Explanatory variables	df	logLik	AICc	ΔAICc	weight	adj. R^2
Trilobatus sacculifer						
sst	3	-491.55	989.81	0.00	0.36	0.20
sst^2	4	-490.75	990.72	0.91	0.23	0.22
sst + abund	4	-491.07	991.36	1.55	0.16	0.20
Globigerinoides ruber						
null	2	-470.04	944.42	0.00	0.26	0.00
abund	3	-468.87	944.42	0.01	0.26	0.07
sst	3	-469.18	945.05	0.63	0.19	0.02
Globigerinoides conglobatus						
null	2	-488.93	982.20	0.00	0.22	0.00
abund	3	-487.85	982.41	0.21	0.20	0.03
sst + abund	4	-486.72	982.65	0.45	0.18	0.03
Globigerinella siphonifera						
sst	3	-464.99	936.72	0.00	0.53	0.20
sst + abund	4	-464.84	938.93	2.22	0.18	0.20
sst^2	4	-464.99	939.22	2.50	0.15	0.18
Neogloboquadrina dutertrei						
null	2	-366.22	736.89	0.00	0.36	0.00
sst	3	-365.72	738.35	1.46	0.17	0.01
abund	3	-365.81	738.53	1.64	0.16	-0.02
Pulleniatina obliquiloculata						
sst	3	-393.81	794.47	0.00	0.52	0.21
sst + abund	4	-393.57	796.62	2.15	0.18	0.22
sst^2	4	-393.77	797.03	2.56	0.15	0.19
Globorotalia menardii						
sst^2 + abund + sst^2:abund	5	-391.06	794.72	0.00	0.46	0.16
sst + abund + sst:abund	6	-390.79	797.39	2.67	0.12	0.15
sst	3	-395.33	797.62	2.90	0.11	0.07
Globorotalia truncatulinoides						
sst^2	4	-373.15	755.91	0.00	0.51	0.22
sst^2 + abund	5	-372.80	758.10	2.20	0.17	0.18
sst^2 + abund + sst^2:abund	5	-373.14	758.78	2.88	0.12	0.19
Globorotalia inflata						
null	2	-232.75	470.20	0.00	0.56	0.00
abund	3	-232.70	472.89	2.69	0.15	-0.05
sst	3	-232.74	472.98	2.79	0.14	-0.06

S6 Boxplots of each species each sample

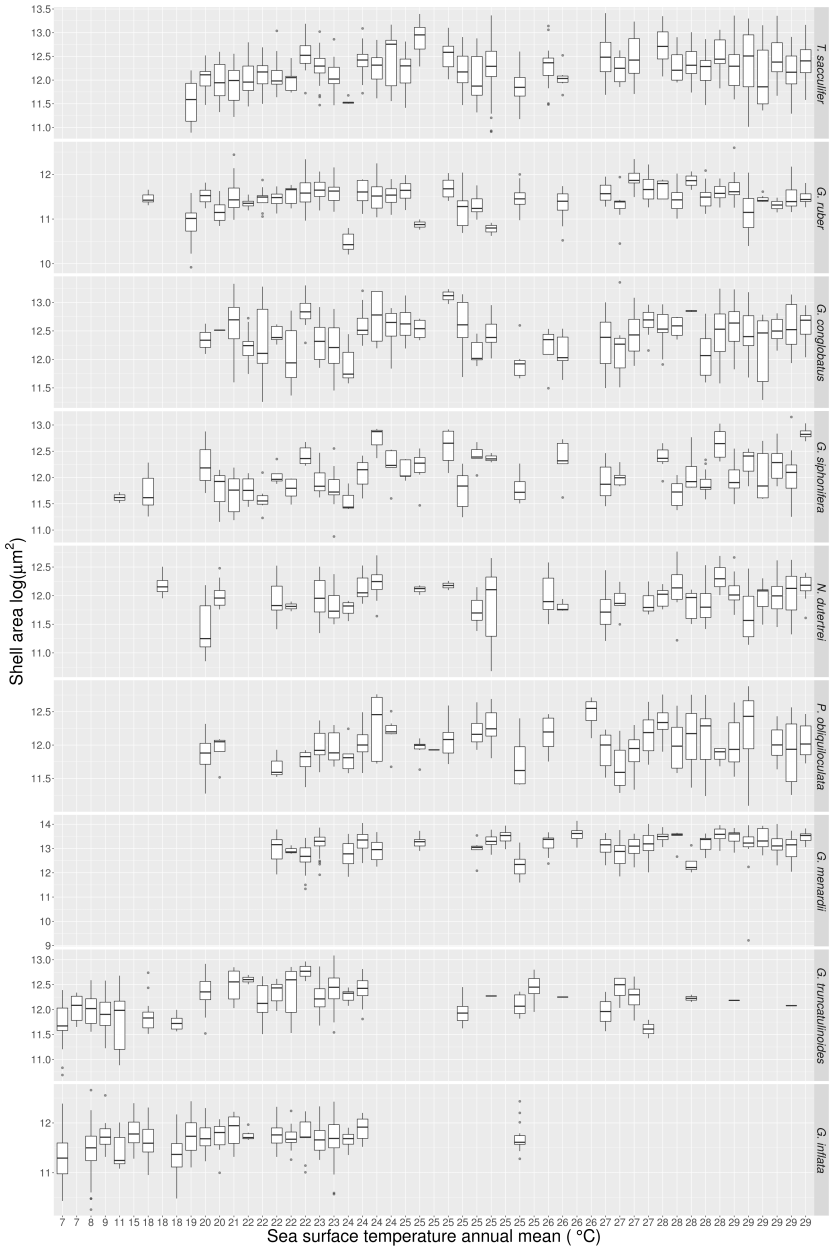

Fig. S3: Shell area within-population variation. Boxplots of individual shell area measurements for each sample for each planktonic foraminifera species. Samples are ordered by sea-surface temperature; note that the x-axis does not increase linearly.

S7 GLM residual plots

Residual plots of the generalised linear model (GLM) with the Gamma logarithmic error function to correct the quadratic shell area distributions. For each species, the dependent response variable was the 95th percentile of the population size distribution whereas the independent explanatory variables were the local relative abundances (median within 300 km distance) and mean annual sea surface temperature.

(a) Trilobatus sacculifer

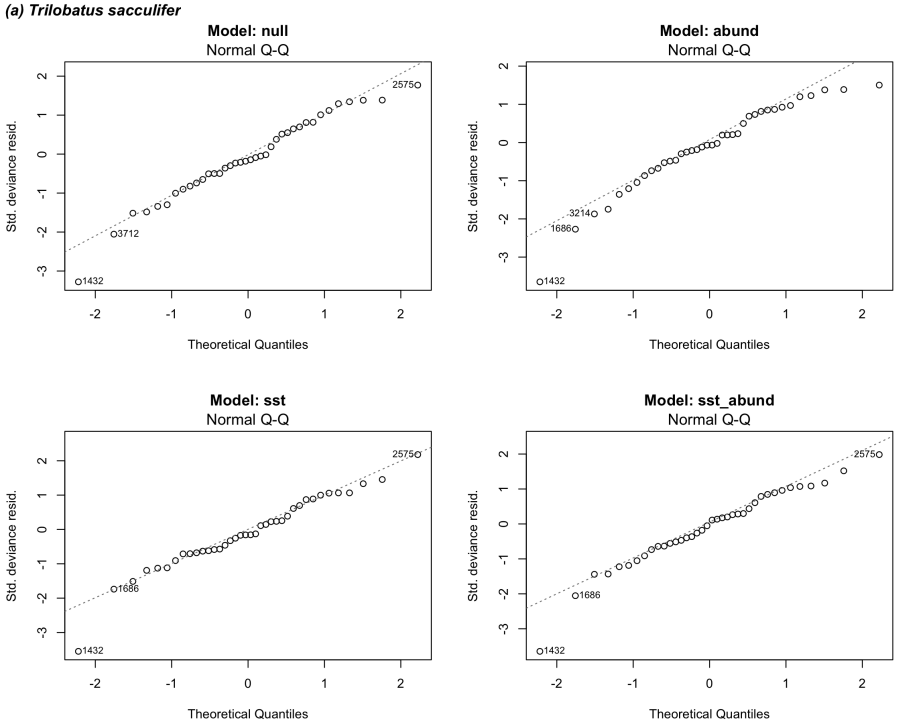

(b) Globigerinoides ruber

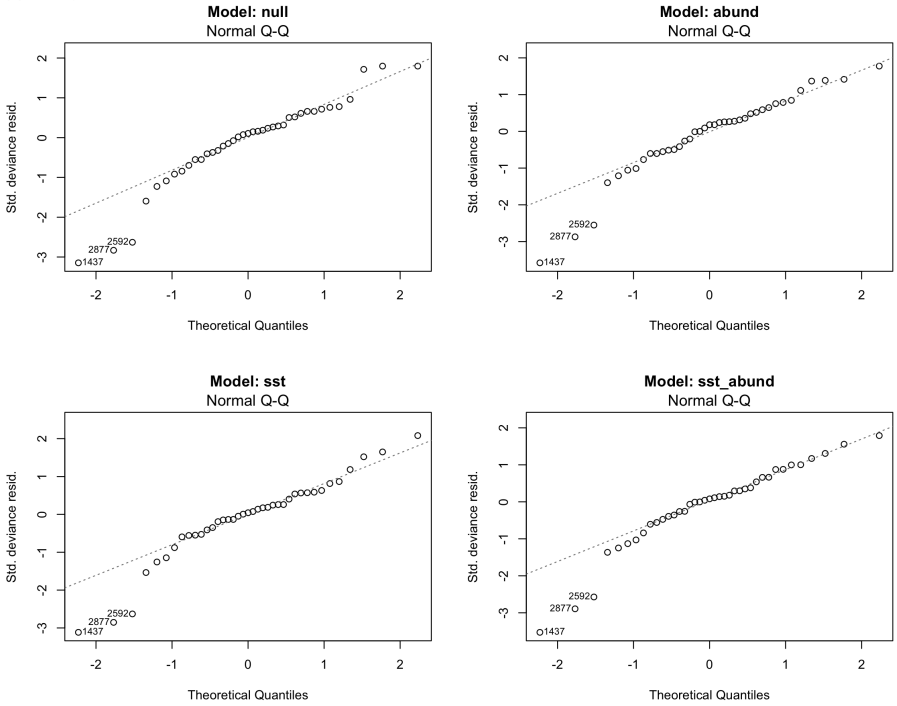

(c) Globigerinoides conglobatus

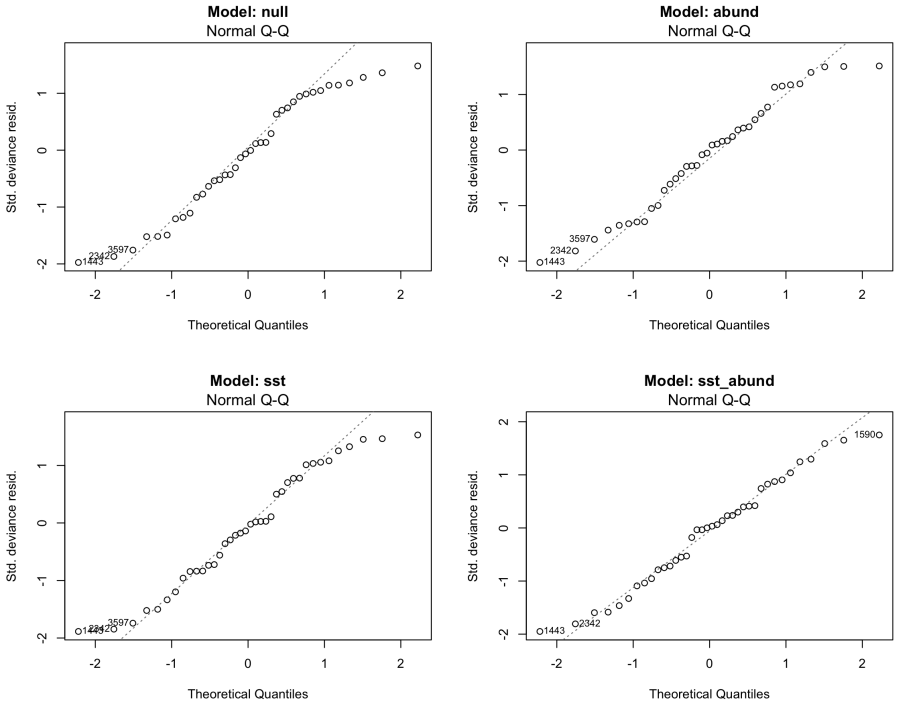

(d) Globigerinella siphonifera

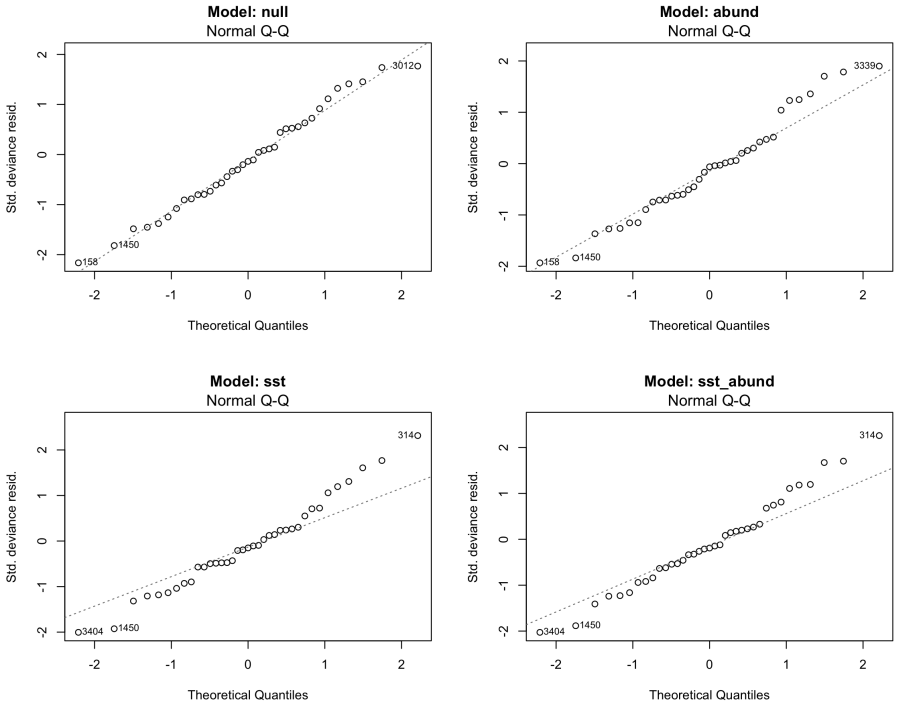

(e) Neogloboquadrina dutertrei

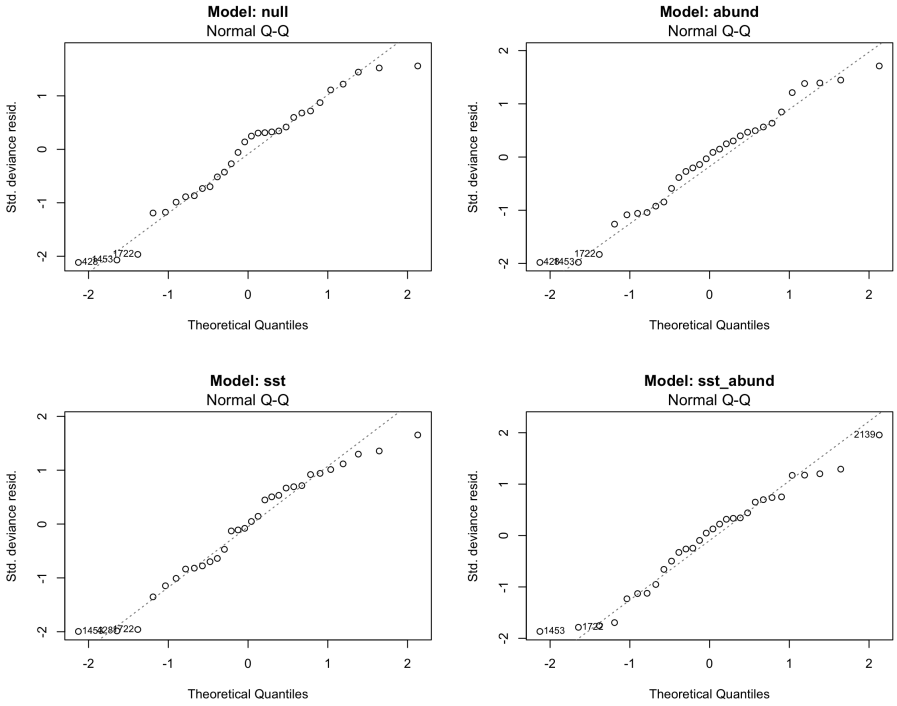

(f) Pulleniatina obliquiloculata

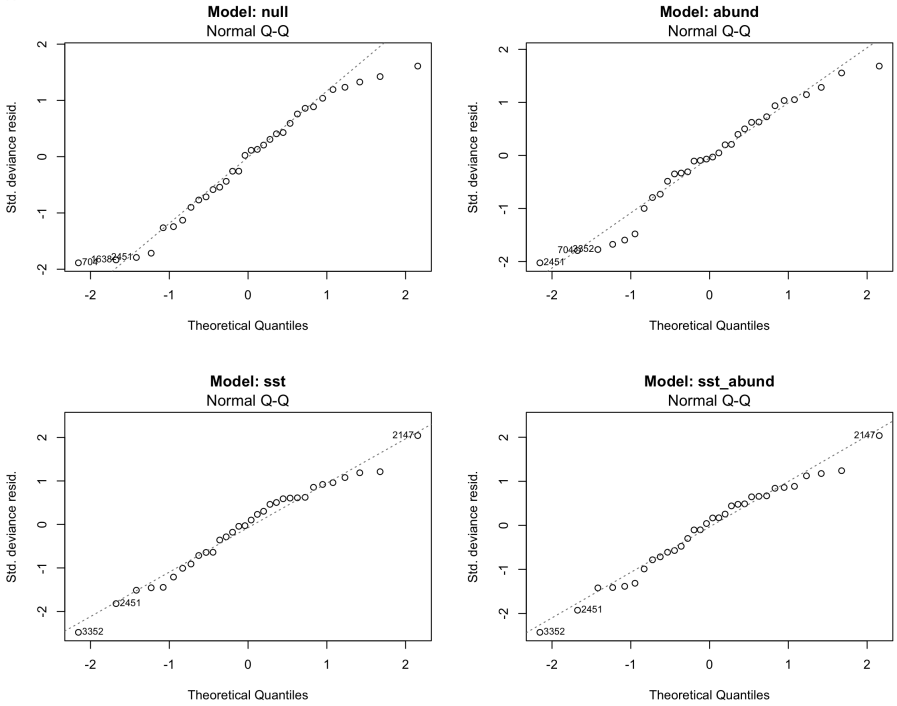

(g) Globorotalia menardii

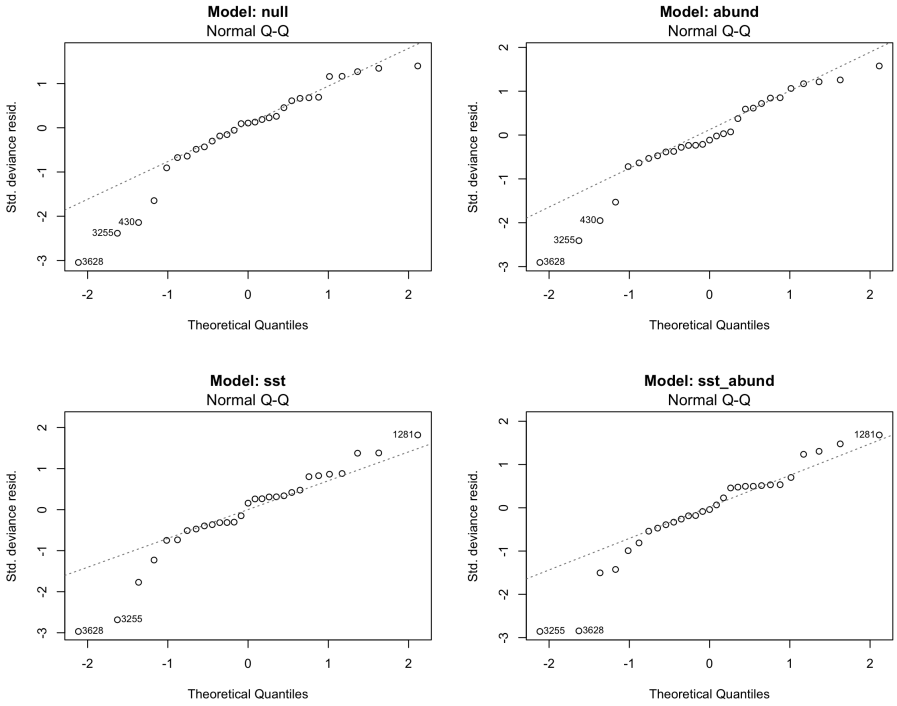

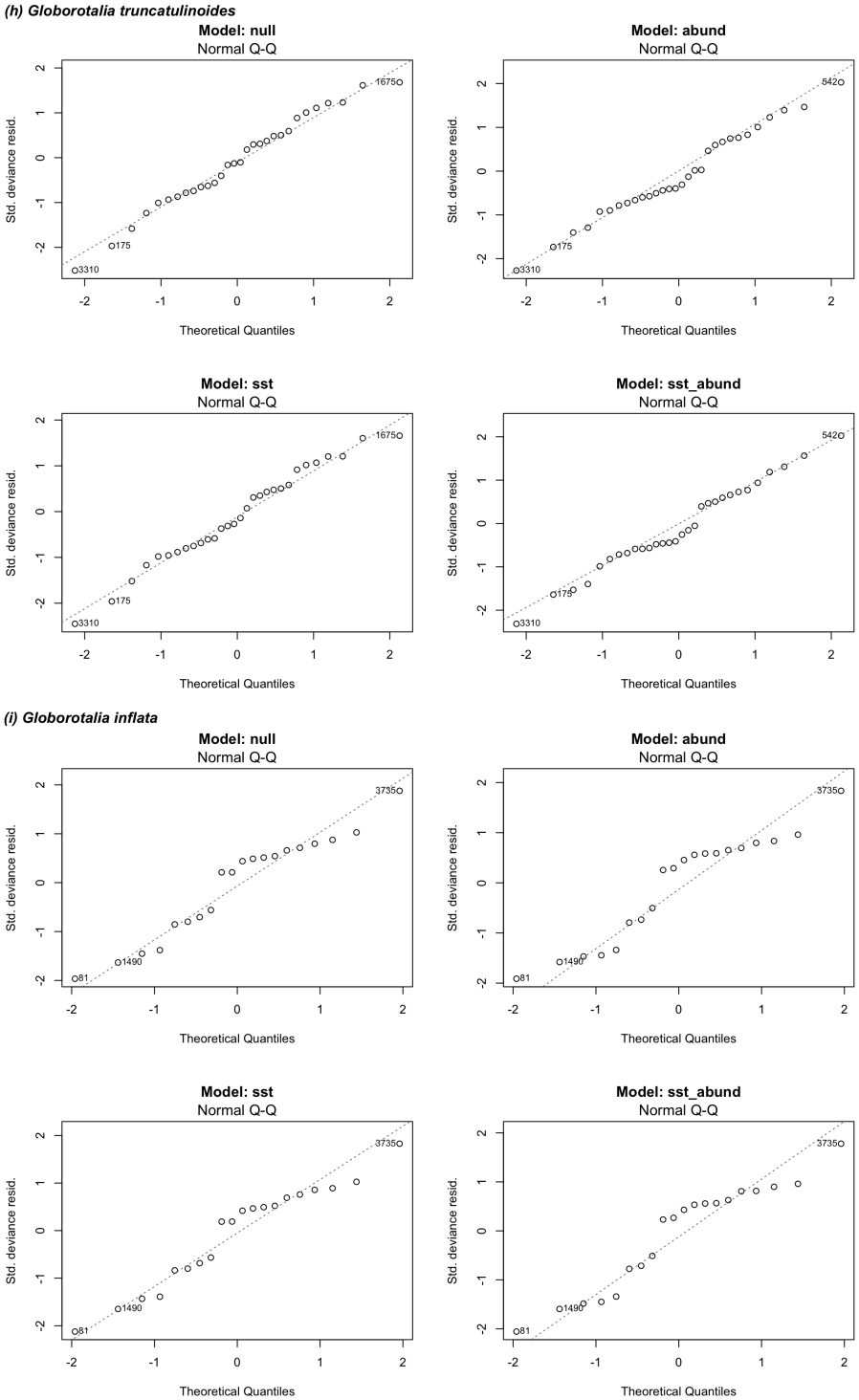

Fig. S4: Generalised linear model residual plots per species. Models: null, abund (relative abundances), sst (mean annual sea surface temperature), and sst_abund (additive effect of sst and abund).